



Recent progress on the flight of dragonflies and damselflies

Toshiyuki Nakata^{a,b}, Per Henningsson^c, Huai-Ti Lin^d and Richard J. Bomphrey^{a*}

^a*Structure and Motion Laboratory, Department of Comparative Biomedical Sciences, Royal Veterinary College, Hatfield, UK;* ^b*Graduate School of Engineering, Chiba University, Chiba, Japan;* ^c*Department of Biology, Lund University, Lund, Sweden;* ^d*Department of Bioengineering, Imperial College London, London, UK*

Remarkable flight performance is key to the survival of adult Odonata. They integrate varied three-dimensional architectures and kinematics of the wings, unsteady aerodynamics, and sensory feedback control in order to achieve agile flight. Therefore, a diverse range of approaches are necessary to understand their flight strategy comprehensively. Recently, new data have been presented in several key areas in Odonata such as measurement of surface topographies, computational fluid dynamic analyses, quantitative flow visualisation using particle image velocimetry, and optical tracking of free flight trajectories in laboratory environments. In this paper, we briefly review those findings alongside more recent studies that have advanced our understanding of the flight mechanics of Odonata still further.

Keywords: Odonata; dragonfly; damselfly; biomechanics; flight; aerodynamics; visual control

Introduction

Flight performance of Odonata greatly affects their survivorship because it directly influences darting hunts, hawking flights, prey selection, interception and capture, predator evasion, and fuel economy during short commutes or long migration journeys. The flight of Odonata, including gliding, hovering, and manoeuvring modes, is achieved by tuning the aerodynamic forces acting on their wings through the control of wing kinematics on the basis of input from multiple sensors. Various architectural components in Odonata wings passively prescribe the posture and shape of the wings. Kinematics of their fore- and hindwings in concert with three-dimensional wing geometries determine aerodynamic performance through the interaction between the wings and the surrounding air. Sensory inputs are monitored to coordinate the motor activities for routine flight control and specialist behavioural modes such as prey capture and conspecific pursuit. Considerable parts of the overall strategy for efficient and robust flight are still unknown because of the multiscale complexities of interactions between morphology, aerodynamics, sensory integration, and motor control.

Toward a comprehensive understanding of the strategy of Odonata, Bomphrey, Nakata, Henningsson, and Lin (2016) have recently presented a wide-ranging description of the biomechanical and neurophysiological aspects of flight alongside new results acquired using a broad suite of modern methods. In this paper, we have briefly summarised the results on the state-of-the-art with some additional updates from more recent studies.

*Corresponding author. Email: rbomphrey@rvc.ac.uk

Structural dynamics of the odonatan wing

The wings of the Odonata are hierarchical structures. Recent research progress, especially those employing computational approaches, have revealed the function of many structural elements. Wing deformation is controlled passively through interactions of the detailed structural elements in the wings. Key elements, including the longitudinal veins, cross-veins, vein-joints (often including flexible resilin sections), the basal complex (defined here as the three-dimensional structure of the proximal part of the wing), nodus, and membrane (Rajabi, Rezasefat, et al., 2016), are particularly important, since the dynamically deforming wing shapes directly affect aerodynamic performance (Young, Walker, Bomphrey, Taylor, & Thomas, 2009). Computational structural dynamic (CSD) analyses on odonatan wings suggest that specific geometries of the vein-joints (Rajabi, Ghoroubi, Darvizeh, Appel, & Gorb, 2016) or the nodus (Rajabi, Ghoroubi, Stamm, Appel, & Gorb, 2017) are responsible for the dorsoventral asymmetry of the wing deformation. While these elements function to control the wing deformation under aerodynamic loads passively during flight, collision with obstacles may lead to excessive loading and structural damage. The rubber-like protein, resilin, present at some vein-joints can considerably reduce the stress concentration in joints when the wings are deformed (Rajabi, Shafiei, Darvizeh, & Gorb, 2016), which may help to mitigate effects of collisions (Mountcastle, Helbling, & Wood, 2019). This is likely to be a secondary function of resilin, following a principal role in facilitating elastic wing deformation during normal flight.

Aerodynamics of gliding and flapping flight

In addition to the wing deformation controlled passively through fluid–structure interactions and inertial bending, the three-dimensional shape and arrangement of the four wings are also important for the flight performance of Odonata. Bomphrey et al. (2016) have performed computational fluid dynamic (CFD) analyses of gliding flight using a low Reynolds number aerodynamic simulator (Liu, 2009) with specific focus on the effect of the corrugated chordwise cross section and the interaction between fore- and hindwings in gliding.

The three-dimensional wing geometries required for this analysis were reconstructed by photographing a series of cross sections illuminated by a laser line projection (Figure 1a). By using the resulting surface topology for CFD analysis, it was found that natural-scale corrugation does not give rise to a dramatic decrease in the lift-to-drag ratio that was observed for corrugations amplitudes that were exaggerated, and larger than those found in nature (Figure 1b, c). Therefore, corrugations can substantially increase wing stiffness without greatly increasing material volume and, moreover, the corrugated structure does not substantially increase aerodynamic costs.

The fore- and hindwing interactions are investigated further by using CFD analyses with the angle of attack, sweep and dihedral angles of the wings relative to the body measured from field photography (Figure 1d). The fore- and hindwings are highly efficient relative to other insect fliers because of their high aspect ratios. By comparing the aerodynamic performance of gliding with fore- and hindwings in tandem against a baseline of fore- and hindwings acting in isolation – i.e. without aerodynamic interactions – Bomphrey et al. (2016) discovered that the dragonflies keep the performance of each wing high by trimming the wing angles to glide efficiently (Figure 1e, f).

In conventional, fixed-wing aircraft, high aspect ratio wings achieve better lift-to-drag ratios than less-slender alternatives. This typically comes at the cost of manoeuvrability because the wing's moment of inertia is increased. However, it is worth noting that this relationship is not always maintained in insects. In genetically modified fruit flies, lines with higher aspect

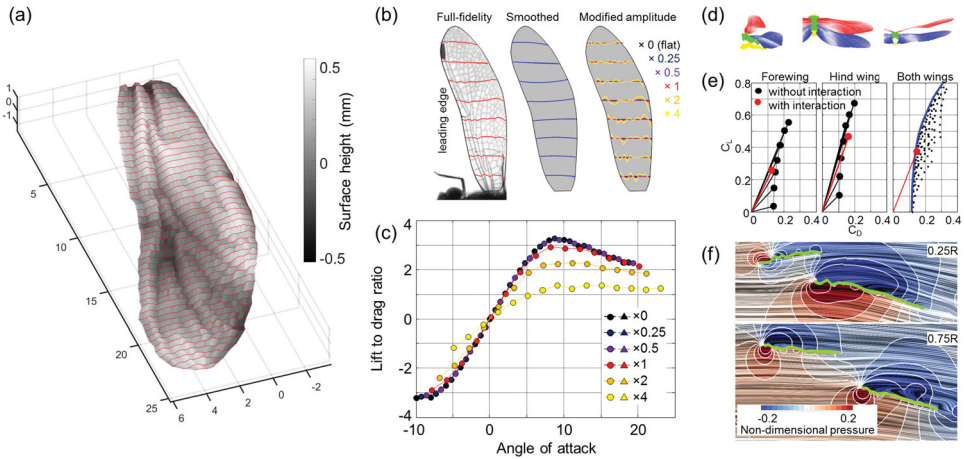


Figure 1. Three-dimensional surface geometry and gliding aerodynamics of dragonfly wings. (a) The complex three-dimensional geometry of the wings for CFD analysis. (b) Selected cross sections of the full-fidelity wing, smoothed wing and the wings with modified amplitude. (c) The lift-to-drag ratio for the exaggerated and reduced corrugation models. (d) Three-dimensional models of the forewing (red), hindwing (blue) and the upper (green) and lower (yellow) surfaces of the thorax. (e) Lift and drag coefficient polars of the fore- and hindwings with (red) or without (black) aerodynamic interactions. (f) The two-dimensional flow structure shown by line integral convolution (LIC) streamlines and pressure distribution contours around the fore- and hindwings at 25% and 75% of wing length. The positive and negative pressure regions of each wing connect with each other, revealing an aerodynamic interaction between the ipsilateral wing pairs. This figure is reproduced from Bomphrey et al. (2016) published under a Creative Commons Attribution License (CC BY 4.0).

ratio wings showed enhanced manoeuvrability, albeit at the cost of a higher power requirement (Ray, Nakata, Henningson, & Bomphrey, 2016). Odonata overcome this physical trade-off of efficiency versus manoeuvrability by operating their four wings independently. For example, damselflies achieve yaw turns by controlling the angle of attack of each wing as well as the flapping velocities of the wings (Zeyghami, Bode-Oke, & Dong, 2017). Their backward flight is enabled by force vectoring, which is based on tilting the stroke plane to adjust the direction of the net aerodynamic forces (Bode-Oke, Zeyghami, & Dong, 2018). Abdominal deflection increases the yaw velocity by reducing the moment of inertia and thus the flight torque required for the manoeuvre (Bode-Oke, Zeyghami, & Dong, 2017b). During take-off, which requires large and finely tuned aerodynamic forces to accelerate in a desired direction, damselflies generate aerodynamic forces that reach three-times body weight, operating each of the four wings at high angles of attack (Bode-Oke, Zeyghami, & Dong, 2017a). Similarly, dragonflies utilise high angles of attack and the synchronous flapping of fore- and hindwings to generate large vertical forces at the beginning of take-off, later switching to lower angles of attack and counter-stroking (out-of-phase) flapping to generate large thrust (Alexander, 1984; Li, Zheng, Pan, & Su, 2018; Thomas, Taylor, Srygley, Nudds, & Bomphrey, 2004). The orientation of aerodynamic forces after the take-off are controlled by adjusting the ratio of downstroke to upstroke duration and the angle of attack of the wings (Shumway, Gabryszuk, & Laurence, 2018).

To support their weight when flapping, the Odonata rely heavily on unsteady aerodynamic mechanisms. In common with many insects, they use a separated flow pattern that delays aerodynamic stall and allows the wing to operate, momentarily, at angles of attack above the steady condition stall angle. During this moment of delayed stall, flow separates from the surface at the leading edge but subsequently re-attaches further back along the chord, ultimately leaving the trailing edge smoothly and satisfying a requirement for the flow on upper and lower surfaces to meet at the sharp trailing edge, known as the Kutta condition. Inside the separation bubble (the volume bounded by the point at which flow detaches and reattaches on the chord), the flow

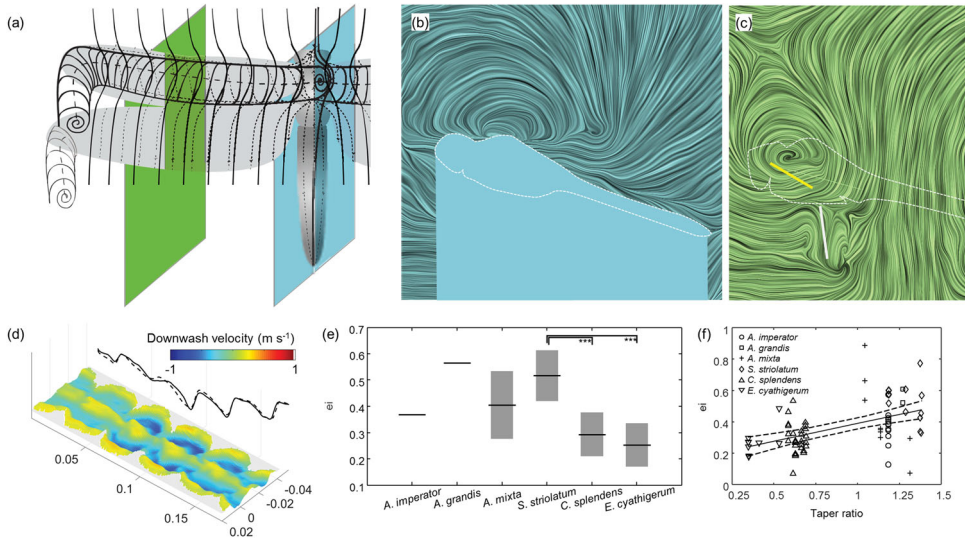


Figure 2. Flapping wing aerodynamics of Odonata. (a) Topology of the leading-edge vortex of a dragonfly. Cross section of the flow at (b) the centreline of the body and (c) approximately 45% of the wing's length from hinge to tip measured by PIV, with instantaneous streamlines visualised by LIC. (d) Example sequence of the time-resolved induced downwash of *Enallagma cyathigerum*. Both the relief and colour represent downwash velocity, with shades in blue/cyan representing downward velocities corresponding to positive lift and shades in red/yellow upward velocities corresponding to negative lift. (e) The span efficiency of each species. Boxes show median values with 95% confidence intervals. Post hoc pairwise ANOVA under a Tukey criterion shows the differences between *Sympetrum striolatum* and two of the Zygoptera are significant ($p < 0.001$). (f) The taper ratio is positively correlated with span efficiency ($p < 0.001$, $R^2 = 0.24$). Solid and dashed lines show the least-squares regression slope with 95% confidence intervals. This figure is reproduced from Bomphrey et al. (2016) published under a Creative Commons Attribution License (CC BY 4.0).

rolls up into a swirling, leading-edge vortex (LEV), allowing the wing to operate at high angles of attack producing remarkably high lift. Quantitative flow visualisations using a laser-based technique called particle image velocimetry (PIV), where the air is seeded with tiny droplets of olive oil, confirmed the qualitative descriptions of the flow topology shown by Bomphrey, Srygley, Taylor, and Thomas (2002) and described in detail by Thomas et al. (2004) (Figure 2a). The typical, counter-stroking, kinematic pattern leads to a cylindrical LEV spanning the thorax (Figure 2b) from forewing tip to forewing tip (Figure 2c), while the hindwing exhibits conventional attached flow. Using their quantitative PIV data, from *Sympetrum striolatum* and *Aeshna mixta*, Bomphrey et al. (2016) have further discovered that: (1) the core diameter of the LEV is substantially greater than the mean chord length of the forewings at all spanwise positions from the centreline to the wing tips; (2) the diameter and circulation increase from root to tip in *A. mixta*; (3) the spanwise contribution to weight support increases from root to tip in both species; and (4) axial velocities at the core of the LEV can be quite strong in either direction (at least during slow forward flight), and is not, therefore, an essential prerequisite of vortex stability during the period of a single half stroke as has been suggested for other insects (Birch & Dickinson, 2001). A recent flow visualisation study by Hefler, Qui, and Shyy (2018) also confirmed the existence of the LEV on the hindwings during free flight, suggesting its dynamics are under the effect of the aerodynamic interactions between fore- and hindwings.

Bomphrey et al. (2016) also used quantitative flow measurements to estimate the efficiency with which lift is generated. Span efficiency (e_i) is the ratio of the power required to generate lift under ideal aerodynamic loading conditions on the wing to the power required in reality: the ideal power divided by the real induced power. Since the power required to generate a given lift is derived from the induced flow velocity, span efficiency can be measured empirically as the

deviation of the downwash velocity profile behind the wings from the theoretical ideal of an even distribution across the span. In the case of a fixed wing, an elliptical planform gives the highest span efficiency by generating an even downwash distribution across the span. Because the local wing velocity increases linearly with distance from the wing hinge, flapping wings should deviate from an elliptical planform and would maximise their efficiency if the wing is broad at the root and tapers towards the tip. The tapering should compensate for the wing's velocity distribution. If we ignore wing twist, or assume that it is comparable across the Odonata, the Anisoptera are, therefore, predicted to perform better than the Zygoptera, since anisopterans have wing shapes with chord lengths that taper toward the wing tip, while zygopterans have wing chord lengths that increase towards the wing tip. We tested this prediction by estimating the span efficiencies for 24 individuals of six Odonata species in free flight in a custom-built wind tunnel, following the protocol of Henningsson and Bomphrey (2013). Figure 2d shows a time series of transects through the downwash at 1 ms intervals for representative examples of *Enallagma cyathigerum*. The colour and relief show the magnitude of the downwash velocity behind the trailing edges of the hindwings, black solid and dashed lines show the vertical excursion of the undulating left and right hindwing tip vortices throughout the sequence. Ensemble-averaged temporal variations in span efficiencies are shown in Figure 2e. As predicted from the difference in the wing shape (Bomphrey et al., 2016), the Zygoptera with narrower wing base have lower span efficiencies (Figure 2e) and span efficiency is strongly correlated with taper ratio (Figure 2f), confirming the relationship between wing planform and aerodynamic efficiency during flapping flight. At the cost of lowered efficiency, the Zygopteran planform shifts the wing's centre of pressure away from the insect's centre of mass, which increases the distance swept by the distal area of the wing. This evolutionary solution might expand the kinematic envelope available and increase the torque that can be generated at the wing hinge when manoeuvring.

Flight performance

Bomphrey et al. (2016) presented two sets of data on the flight performance of Odonata, aiming at providing standardised baseline data and showing quantitative differences in an indoor flight performance during cruising, predatory and territorial escort flights. As an example, Figure 3a–c shows the speed, turn rate and turn radius of nine species of Odonata in an indoor flight arena with plain background, acquired using calibrated stereo-cameras (following the protocol detailed previously; Henningsson & Bomphrey, 2013; Ray, et al., 2016). Statistical analyses suggested that: (1) the Zygoptera tended to fly more slowly than the Anisoptera, but the majority of species preferred to fly between 1 and 2 m s⁻¹; (2) turn rates can reach up to 1000 deg s⁻¹ in several species; (3) turn radius were mostly less than 0.5 m. Another set of probability density functions in Figure 3d–f show the speed, turn rate and turn radius of *Plathemis lydia* during cruising, predatory and territorial flights, recorded in a fully texturised realistic indoor arena as described by Mischiati et al. (2015). It is clear that the predatory and territorial flights are more demanding than cruising flight; territorial flight and prey interception flight exhibited higher speeds (Figure 3d) and also more rapid turns (Figure 3e). Territorial flights in our experimental observations were faster than the predatory flights, but the turn radius of the predatory flights was slightly tighter than those observed during territorial flights (Figure 3f). We do not expect these behaviours to exhibit the full repertoire of each species, but the standardisation within our well-defined and repeatable settings is useful for benchmarking a conservative flight performance envelope. The metrics provided in this study highlight coarse interspecies variability for future investigations into comparative flight performance.

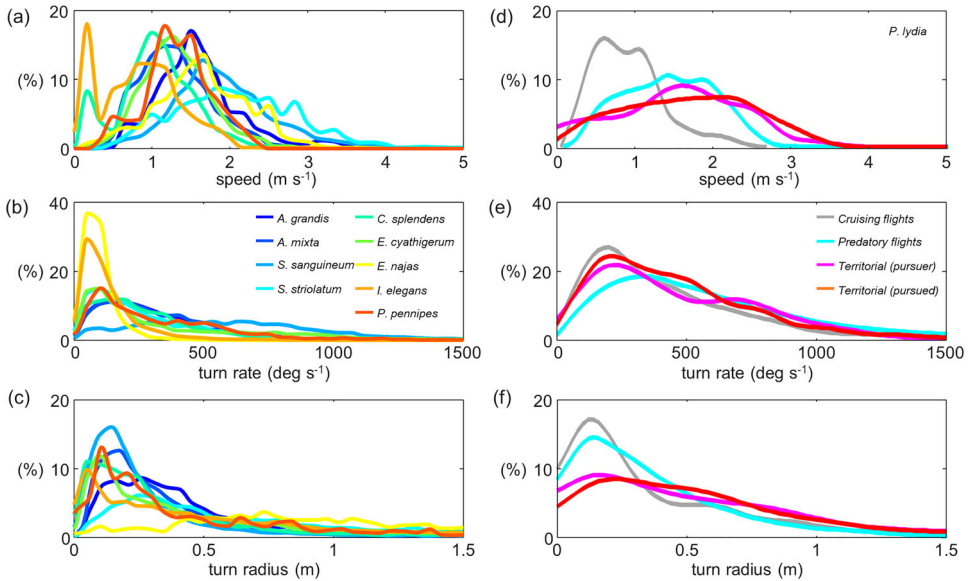


Figure 3. Flight performance of Odonata. (a) Speed, (b) turn rate, and (c) turn radius of nine species of Odonata. (d) Speed, (e) turn rate and (f) turn radius of *Plathemis lydia* during cruising, hunting and territorial flights. This figure is reproduced from Bomphrey et al. (2016) published under a Creative Commons Attribution License (CC BY 4.0).

Neurophysiology of dragonfly vision

The dragonfly's impressive visual abilities have motivated numerous studies on the neurophysiology of small target detections. The most notable ones can be dated back to the 1980s with the discovery of the target selective descending neurons (TSDNs) that transmit target movement information from the visual centre in the head to the motor centre in the thorax (Olberg, 1986). Later, the small target motion detectors (STMDs) were discovered in the third visual neuropil, lobula (O'Carroll, 1993). Both classes of neurons respond to small shadows moving in a relatively wide area of the visual field. TSDNs were assumed to be the downstream neurons of STMDs for a long time, yet a direct evidence has never been established. The signal encoding properties of TSDNs have been a subject of study (Adelman, Bialek, & Olberg, 2003; Gonzalez-Bellido, Peng, Yang, Georgopoulos, & Olberg, 2013), yet the detailed characterisation remains incomplete. Ongoing work aims to establish the functional role of TSDNs and the signal transformation from the visual system.

Behavioural studies and physiological studies go hand-in-hand to advance our understanding of dragonfly vision. Through precise measurement of dragonfly head movement during repeated prey interception flights, Mischiati et al. (2015) established the predictive nature of dragonfly prey interception behaviour. Given the visuomotor latency, the rapid aerial interception cannot be implemented purely via a fast reactive control mechanism. The way the dragonfly's head cancels expected target movement during flight demonstrates the existence of a prey model and the role of predictive control. This observation was reinforced by the discovery of a strong predictive neural facilitation in STMDs (Wiederman, Fabian, Dunbier, & O'Carroll, 2017). As the target moves across the visual receptive field of a STMD neuron, the sensitivity of target detection in front of the current target position is enhanced by over 50%. This demonstrates that the visual system indeed has the ability to anticipate the future target location. Contrary to earlier suggestions (Olberg, Worthington, Fox, Bessette, & Loosemore, 2005), dragonflies do not have independent estimation of prey distance. From scrutinising visual parameters of the dragonfly's

prey selection, we have shown that target selection is highly tuned to the fine target movement qualities and the interception flight dynamics (Lin & Leonardo, 2017). This selection might be correlated but not purely driven by target detection limits. Dragonflies have incredible sensitivity to detecting targets that are smaller than single photoreceptor. A recent study compared the photoreceptor sensitivity to small targets in dragonflies, hoverflies, honey bee drones, and blowflies (Rigosi, Wiederman, & O'Carroll, 2017). The result confirmed a similar subpixel target detection level ($< 0.2^\circ$ target) as reported by the target selection behaviour study (Lin & Leonardo, 2017).

Finally, a recent study compared visual motion detection responses in dragonflies and macaque monkeys (Nitzany et al., 2017). It shows that both systems respond to some motion cues that cannot be explained by the classic Hassenstein–Reichardt model. With the discovery of a class of wide-field sensitive neurons in the dragonfly lobula (Evans, O'Carroll, Fabian, & Wiederman, 2019), we expect dragonflies to serve as an alternative model system for understanding the fundamental mechanism of motion detection.

Concluding remarks

The use of computational structural and fluid dynamic analysis has separately driven progress toward a more complete understanding of the functional morphology of the wings of the Odonata and their flight mechanics. Computational analyses revealed that wing deformation is passively controlled by the hierarchical architecture of odonatan wings, but its effect on flight performance is yet to be resolved. This is because the coupling of passive wing deformation and unsteady aerodynamics is not yet taken into account. Nor is it well understood how the steering muscles modify wing shape during cyclical flapping or manoeuvres. Wing deformations affect the sensory encoding of mechanosensors located on the veins but we do not yet know how wing deformations are monitored by the flight controller. It is also not yet clear how body rotations affect wing deformations and, thus, how mechanosensory signals could be used in flight control in turbulent atmospheric conditions. There is a growing body of work in the context of moth wings acting as gyroscopic sensors (Pratt, Deora, Mohren, & Daniel, 2017) analogous to the well-studied function of halteres in Diptera. Therefore, we must work towards a comprehensive wing structural model coupled with the surrounding fluid dynamics. With this model we can begin to understand the functional significance of each structural element and dissect the inertial and aerodynamic components in the wing mechanosensory system. Current advances in computational modelling methods certainly help towards this comprehensive fluid–structure interaction analysis. Aerodynamic experiments on real animals, where wing surfaces and flow velocities close to the wings can be measured simultaneously, are now possible and will be vital for computational model validation (Bomphrey & Godoy-Diana, 2018; Nila et al., 2016). The combination of such empirical and computational approaches would add strength and robustness to the results.

Several more key areas that will advance our understanding of the flight strategy of the Odonata were identified by Bomphrey et al. (2016). The behavioural repertoire of the Odonata is diverse, and we must develop new approaches that allow high throughput, high-quality wing kinematics measurements (Koehler, Liang, Gaston, Wan, & Dong, 2012; Walker, Thomas, & Taylor, 2009). The use of artificial targets with prescribed perturbation will allow us to formulate behavioural models by artificially eliciting predictable and repeatable flight responses (Fabian, Sumner, Wardill, Rossoni, & Gonzalez-Bellido, 2018; Mischiati, et al., 2015). The wings are, of course, driven by the flight motor and wing hinge; in order to understand the interplay of these musculoskeletal elements during the various behaviours, a combination of tethered flight and wireless recording of the flight muscles would be very useful.

Comprehensive analyses are extremely challenging, but flight in Odonata represents a fine example of a natural aerial system in which complex wing morphology, unsteady aerodynamics and neural feedback control are integrated to achieve extraordinary flight behaviour. Ongoing work focuses on revealing the neural representation of wing aeroelasticity. Understanding such a system can inspire the development of novel agile micro aerial vehicles with sophisticated “fly-by-feel” control systems that use mechanosensory information about loads on the wing surface in the flight controller. Finally, while behavioural and neurophysiological studies continue to work synergistically to advance our understanding of flight control, we believe it is necessary to retain biomechanics as a fundamental link between the two, to set each in context, and to answer the proximate questions of flight in the Odonata and other insects.

Funding

This work was partly supported by JSPS KAKENHI [JP18H05468] to T.N, Swedish research council [2013-4838 and 2018-04292] to P.H., Biotechnology and Biological Sciences Research Council [BB/R002509/1] to H.T.L and [BB/R002657/1] to R.J.B.

References

- Adelman, T. L., Bialek, W., & Olberg, R. M. (2003). The information content of receptive fields. *Neuron*, *40*(4), 823–833. doi:10.1016/s0896-6273(03)00680-9
- Alexander, D. E. (1984). Unusual phase relationships between the forewings and hindwings in flying dragonflies. *Journal of Experimental Biology*, *109*, 379–383.
- Birch, J. M., & Dickinson, M. H. (2001). Spanwise flow and the attachment of the leading-edge vortex in insect wings. *Nature*, *412*, 729–733. doi:10.1038/35089071
- Bode-Oke, A. T., Zeyghami, S., & Dong, H. (2017a). Aerodynamics and flow features of a damselfly in takeoff flight. *Bioinspiration & Biomimetics*, *12*(5), 056006. doi:10.1088/1748-3190/aa7f52
- Bode-Oke, A. T., Zeyghami, S., & Dong, H. (2017b). Optimized body deformation in dragonfly maneuvers. *arXiv*, 1707.07704.
- Bode-Oke, A. T., Zeyghami, S., & Dong, H. (2018). Flying reverse: kinematics and aerodynamics of a dragonfly in backward free flight. *Journal of the Royal Society Interface*, *15*, 20180102. doi:10.1098/rsif.2018.0102
- Bomphrey, R. J., & Godoy-Diana, R. (2018). Insect and insect-inspired aerodynamics: Unsteadiness, structural mechanics and flight control. *Current Opinion in Insect Science*, *30*, 26–32. doi: 10.1016/j.cois.2018.08.003
- Bomphrey, R. J., Nakata, T., Henningson, P., & Lin, H. T. (2016). Flight of the dragonflies and damselflies. *Philosophical Transactions of the Royal Society B*, *371*(1704), 20150389. doi:10.1098/rstb.2015.0389
- Bomphrey, R. J., Srygley, R. B., Taylor, G. K., & Thomas, A. L. R. (2002). Visualising the flow around insect wings. *Physics of Fluids*, *14*, S4. doi:10.1063/1.4739193
- Evans, B., J., O’Carroll, D. C., Fabian, J. M., & Wiederman, S. D. (2019). Differential tuning to visual motion allows robust encoding of optic flow in the dragonfly. *Journal of Neuroscience*, *39*(41), 8051–8063. doi:10.1523/JNEUROSCI.0143-19.2019
- Fabian, S. T., Sumner, M. E., Wardill, T. J., Rossoni, S., & Gonzalez-Bellido, P. T. (2018). Interception by two predatory fly species is explained by a proportional navigation feedback controller. *Journal of the Royal Society Interface*, *15*, 20180466. doi:10.1098/rsif.2018.0466
- Gonzalez-Bellido, P. T., Peng, H., Yang, J., Georgopoulos, A. P., & Olberg, R. M. (2013). Eight pairs of descending visual neurons in the dragonfly give wing motor centers accurate population vector of prey direction. *Proceedings of the National Academy of Sciences*, *110*(2), 696–701. doi:10.1073/pnas.1210489109
- Hefler, C., Qui, H., & Shyy, W. (2018). Aerodynamic characteristics along the wing span of a dragonfly *Pantala flavescens*. *Journal of Experimental Biology*, *221*, jeb171199. doi:10.1242/jeb.171199
- Henningson, P., & Bomphrey, R. J. (2013). Span efficiency in hawkmoths. *Journal of the Royal Society Interface*, *10*(84), 20130099. doi:10.1098/rsif.2013.0099
- Koehler, C., Liang, Z., Gaston, Z., Wan, H., & Dong, H. (2012). 3D reconstruction and analysis of wing deformation in free-flying dragonflies. *Journal of Experimental Biology*, *215*, 3018–3027. doi:10.1242/jeb.069005
- Li, Q., Zheng, M., Pan, T., & Su, G. (2018). Experimental and numerical investigation on dragonfly wing and body motion during voluntary take-off. *Scientific Reports*, *8*, 1011. doi:10.1038/s41598-018-19237-w
- Lin, H. T., & Leonardo, A. (2017). Heuristic rules underlying dragonfly prey selection and interception. *Current Biology*, *27*, 1124–1137. doi:10.1016/j.cub.2017.03.010
- Liu, H. (2009). Integrated modeling of insect flight: from morphology, kinematics to aerodynamics. *Journal of Computational Physics*, *228*, 439–459. doi:10.1016/j.jcp.2008.09.020
- Mischianti, M., Lin, H. T., Herold, P., Imler, E., Olberg, R., & Leonardo, A. (2015). Internal models direct dragonfly interception steering. *Nature*, *517*(7534), 333–338. doi:10.1038/nature14045

- Mountcastle, A. M., Helbling, E. F., & Wood, R. J. (2019). An insect-inspired collapsible wing hinge dampens collision-induced body rotation rates in a microrobot. *Journal of the Royal Society Interface*, *16*, 20180618. doi:10.1098/rsif.2018.0618
- Nila, A., Phillips, N., Bomphrey, R. J., Bleischwitz, R., de Kat, R., & Ganapathisubramani, B. (2016) *Optical measurements of fluid–structure interactions for the description of nature-inspired wing dynamics*. Paper presented at the 2016 RAeS Applied Aerodynamics Conference, Bristol, UK.
- Nitzany, E., Menda, G., Shamble, P. S., Golden, J. R., Hu, Q., Hoy, R. R., & Victor, J. (2017). Neural computations combine low-and high-order motion cues similarly, in dragonfly and monkey. *bioRxiv*, 240101. doi:10.1101/240101
- O’Carroll, D. (1993). Feature-detecting neurons in dragonflies. *Nature*, *362*, 541. doi:10.1038/362541a0
- Olberg, R. M. (1986). Identified target-selective visual interneurons descending from the dragonfly brain. *Journal of Comparative Physiology A*, *159*, 827–840. doi:10.1007/BF00603736
- Olberg, R. M., Worthington, A. H., Fox, J. L., Bessette, C. E., & Loosemore, M. P. (2005). Prey size selection and distance estimation in foraging adult dragonflies. *Journal of Comparative Physiology A*, *191*(9), 791–797. doi:10.1007/s00359-005-0002-8
- Pratt, B., Deora, T., Mohren, T., & Daniel, T. (2017). Neural evidence supports a dual sensory-motor role for insect wings. *Proceedings of the Royal Society B*, *284*(1862), 20170969. doi:10.1098/rspb.2017.0969
- Rajabi, H., Ghoroubi, N., Darvizeh, A., Appel, E., & Gorb, S. N. (2016). Effects of multiple vein microjoints on the mechanical behaviour of dragonfly wings: numerical modelling. *Royal Society Open Science*, *3*, 150610. doi:10.1098/rsos.150610
- Rajabi, H., Ghoroubi, N., Stamm, K., Appel, E., & Gorb, S. N. (2017). Dragonfly wing nodus: A one-way hinge contributing to the asymmetric wing deformation. *Acta Biomaterialia*, *60*, 330–338. doi:10.1016/j.actbio.2017.07.034
- Rajabi, H., Rezasefat, M., Darvizeh, A., Dirks, J.-H., Eshghi, S., Shafiei, A., Mirzababaei Mostofi, T., & Gorb, S. N. (2016). A comparative study of the effects of constructional elements on the mechanical behaviour of dragonfly wings. *Applied Physics A*, *122*, 19. doi:10.1007/s00339-015-9557-6
- Rajabi, H., Shafiei, A., Darvizeh, A., & Gorb, S. N. (2016). Resilin microjoints: a smart design strategy to avoid failure in dragonfly wings. *Scientific Reports*, *6*, 39039. doi:10.1038/srep39039
- Ray, R. P., Nakata, T., Henningsson, P., & Bomphrey, R. J. (2016). Enhanced flight performance by genetic manipulation of wing shape in *Drosophila*. *Nature Communications*, *7*, 10851. doi:10.1038/ncomms10851
- Rigosi, E., Wiederman, S. D., & O’Carroll, D. C. (2017). Photoreceptor signalling is sufficient to explain the detectability threshold of insect aerial pursuers. *Journal of Experimental Biology*, *220*, 4364–4369. doi:10.1242/jeb.166207
- Shumway, N. M., Gabryszuk, M., & Laurence, S. J. (2018) *Flapping tandem-wing aerodynamics: dragonflies in steady forward flight*. Paper presented at the 2018 AIAA Aerospace Sciences Meeting, Florida. doi:10.2514/6.2018-1290
- Thomas, A. L. R., Taylor, G. K., Srygley, R. B., Nudds, R. L., & Bomphrey, R. J. (2004). Dragonfly flight: free-flight and tethered flow visualizations reveal a diverse array of unsteady lift-generating mechanisms, controlled primarily via angle of attack. *Journal of Experimental Biology*, *207*, 4299–4323. doi:10.1242/jeb.01262
- Walker, S. M., Thomas, A. L. R., & Taylor, G. K. (2009). Photogrammetric reconstruction of high-resolution surface topographies and deformable wing kinematics of tethered locusts and free-flying hoverflies. *Journal of the Royal Society Interface*, *6*, 351–366. doi:10.1098/rsif.2008.0245
- Wiederman, S. D., Fabian, J. M., Dunbier, J. R., & O’Carroll, D. C. (2017). A predictive focus of gain modulation encodes target trajectories in insect vision. *eLife*, *6*, e26478. doi:10.7554/eLife.26478
- Young, J., Walker, S. M., Bomphrey, R. J., Taylor, G. K., & Thomas, A. L. R. (2009). Details of insect wing design and deformation enhance aerodynamic function and flight efficiency. *Science*, *325*, 1549–1552. doi:10.1126/science.1175928
- Zeyghami, S., Bode-Oke, A. T., & Dong, H. (2017). Quantification of wing and body kinematics in connection to torque generation during damselfly yaw turn. *Science China Physics, Mechanics & Astronomy*, *60*(1), 014711. doi:10.1007/s11433-016-0302-5